AD-A131 785 CLUSTERING AND ORDERING IN III-V ALLOYS(U) WASHINGTON UNIV ST LOUIS MO SEMICONDUCTOR RESEARCH LAB C M WOLFE ET AL. 31 JUL 83 WU/SRL-59583-1 1/1

UNCLASSIFIED AFOSR-TR-83-0715 AFOSR-82-0231 F/G 20/2 NL

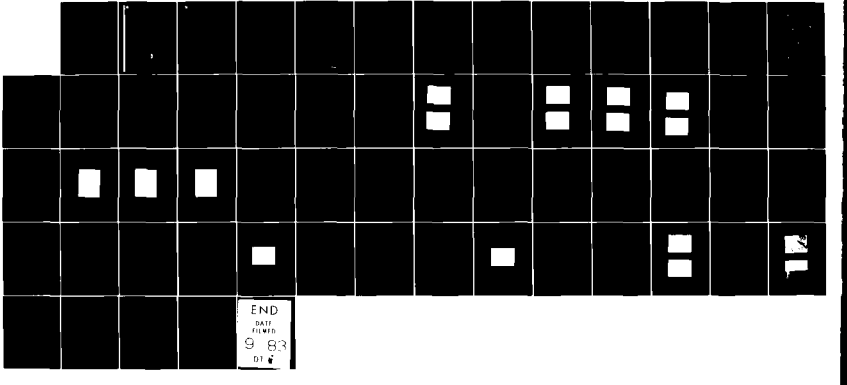

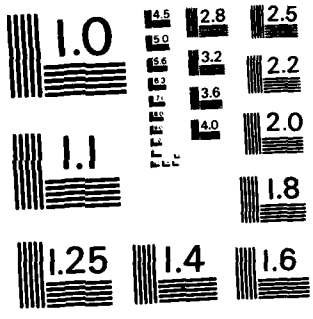

CLUSTERING AND ORDERING IN III-V ALLOYS

SEMICONDUCTOR RESEARCH LABORATORY

Washington University

Saint Louis, Missouri 63130

31 July 1983

ANNUAL SCIENTIFIC REPORT NO. WU/SRL-59583-1

1 June 1982 to 31 May 1983

Air Force Office of Scientific Research
Building 410
Bolling Air Force Base, DC20332

Approved for public release; distribution unlimited.

Grant No. AFOSR-82-0231

WASHINGTON UNIVERSITY IN ST. LOUIS

CLUSTERING AND ORDERING IN III-V ALLOYS

SEMICONDUCTOR RESEARCH LABORATORY

Washington University

Saint Louis, Missouri 63130

31 July 1983

ANNUAL SCIENTIFIC REPORT NO. WU/SRL-59583-1

1 June 1982 to 31 May 1983

Air Force Office of Scientific Research
Building 410
Bolling Air Force Base, DC20332

Grant No. AFOSR-82-0231

Unclassified

SECURITY CLASSIFICATION OF THIS PAGE (When Data Entered)

REPORT DOCUMENTATION PAGE		READ INSTRUCTIONS BEFORE COMPLETING FORM
1. REPORT NUMBER AFOSR-TR- 83-0715	2. GOVT ACCESSION NO. A131785	3. RECIPIENT'S CATALOG NUMBER
4. TITLE (and Subtitle) Clustering and Ordering in III-V Alloys		5. TYPE OF REPORT & PERIOD COVERED Annual 1 Jun 82-31 May 83
		6. PERFORMING ORG. REPORT NUMBER WU/SRL-59583-1
7. AUTHOR(s) C.M. Wolfe, M.W. Muller, G.A. Davis, S. Julie Hsieh, K.A. Salzman		8. CONTRACT OR GRANT NUMBER(s) AFOSR-82-0231
9. PERFORMING ORGANIZATION NAME AND ADDRESS Washington University Box 1127 St. Louis, MO 63130		10. PROGRAM ELEMENT, PROJECT, TASK AREA & WORK UNIT NUMBERS 61102F 2306/B1
11. CONTROLLING OFFICE NAME AND ADDRESS Air Force Office of Scientific Research Building 410 Bolling AFB, DC 20332		12. REPORT DATE 31 Jul 83
		13. NUMBER OF PAGES 53
14. MONITORING AGENCY NAME & ADDRESS(if different from Controlling Office)		15. SECURITY CLASS. (of this report) Unclassified
		15a. DECLASSIFICATION/DOWNGRADING SCHEDULE

16. DISTRIBUTION STATEMENT (of this Report)

Approved for public release; distribution unlimited.

17. DISTRIBUTION STATEMENT (of the abstract entered in Block 20, if different from Report)

18. SUPPLEMENTARY NOTES

19. KEY WORDS (Continue on reverse side if necessary and identify by block number)

$In_xGa_{1-x}P$, GaAs, $ZnSnP_2$, epitaxial growth, crystal structure, sphalerite, chalcopyrite, heterostructures.

20. ABSTRACT (Continue on reverse side if necessary and identify by block number)

The III-V semiconducting alloys are typically grown by epitaxial techniques at temperatures where, in the absence of substrate effects, they are thermodynamically unstable. This can result in problems associated with clustering of like atoms or ordering of unlike atoms. Long-range ordering could yield interesting III-V ternary compounds.

Several concepts are discussed which could reduce clustering and promote long-range ordering in III-V alloys. Recent results

DD FORM 1 JAN 73 1473 EDITION OF 1 NOV 65 IS OBSOLETE

Unclassified

SECURITY CLASSIFICATION OF THIS PAGE (When Data Entered)

20. Abstract (Continued)

indicate that the local atomic structure in $Ga_xIn_{1-x}As$ is chalcopyrite-like and that long-range ordering may be thermodynamically feasible. Kinetically, it is suggested that growth on {211} substrates could promote long-range order.

These concepts were most easily tested in chalcopyrite-on-sphalerite epitaxy where long-range ordering is reflected in the ternary chalcopyrite compound. Experiments on epitaxially grown layers of $ZnSnP_2$ on GaAs substrates indicate that antiphase boundaries are reduced for {110} growth and eliminated for {211} growth. The elimination of antiphase boundaries corresponds to essentially complete order.

Work on the growth of lattice-matched $Ga_xIn_{1-x}P$ on GaAs indicates different effective segregation coefficients for different orientations. Preliminary results suggest that growth on {111} substrates is less stable than on {110} substrates. Growth of $Ga_xIn_{1-x}P$ on {211} substrates is currently under investigation.

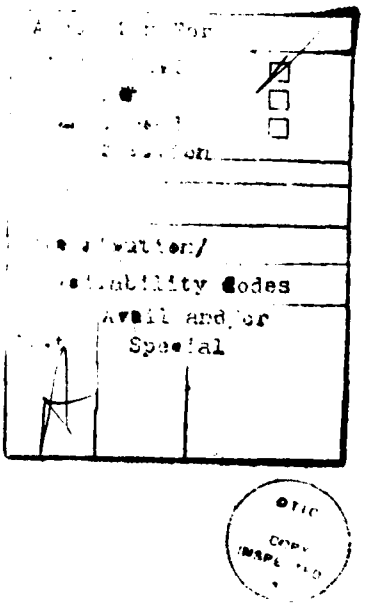

TABLE OF CONTENTS

1. INTRODUCTION

Although there is substantial interest in III-V semiconductor alloys for electronic and optoelectronic devices, relatively little is known about the distribution of atoms in these materials or the effects of non-random distributions on device performance. In many of these alloys, however, non-random distributions of atoms are expected to be important from thermodynamic considerations. This is particularly true at the low temperatures commonly used for epitaxial growth. The available evidence suggests that short-range clustering of like atoms or short-range ordering of unlike atoms can produce device problems such as excess noise and leakage current, premature voltage breakdown, and lower carrier mobilities. Long-range ordering of unlike atoms, however, could potentially yield III-V ternary compounds with properties superior to their parent alloys. In epitaxial growth, substrate effects such as lattice match and nonequivalent sublattice sites are expected to have a strong influence on these phenomena. Also, two of the important III-V alloys, $Ga_xIn_{1-x}P$ and $Ga_xIn_{1-x}As$, can be epitaxially grown lattice matched to GaAs and InP, respectively, at compositions near the point of greatest ordering probability. The objective of this work is to investigate various aspects of clustering and ordering in these materials.

2. CLUSTERING AND ORDERING PHENOMENA

This section is directed at elucidating the growth conditions for these two electronically useful alloys that will prevent clustering, and at attempting to identify factors that would favor the growth of ordered material.

2.1 THERMODYNAMIC ASPECTS

As indicated above the alloys chosen for this study, $Ga_xIn_{1-x}P$ and $Ga_yIn_{1-y}As$, can be grown lattice-matched at compositions near $x \simeq y \simeq 0.5$ on GaAs and InP substrates respectively, but it still is not known with certainty whether they are actually thermodynamically stable at the growth temperature. A recent analysis [1] concludes that both alloys should exhibit miscibility gaps, with critical temperatures, T_c, of 973K and 735K for the phosphide and arsenide, respectively. This contradicts an earlier calculation by the same author [2] which results in a negative value for the heat of mixing of $Ga_{0.5}In_{0.5}P$ and so would predict a transition to long range order, albeit with a lower critical temperature. Both these results, which are quite representative of the current state of the theory, are based on the measured compositional dependence of bandgaps and bandwidths, and on the presumed relation between these quantities and the energy of formation of the compound; and they are equally reliable. Which is only to say that theory is not an infallible guide in these problems.

A heartening contrast is furnished by some quite unambiguous experimental findings that are germane to this work. The first is the phenomenon of "lattice latching" [3], which constrains the epitaxial growth of an alloy to the composition which lattice-matches the substrate, near $x = y = 0.5$ in the systems we are studying. Specifically, the lattice-matched, unstrained alloy grows not only from a melt of the exactly correct liquidus composition, but from a range of values around this composition. The interpretation of this phenomenon in terms of mismatch strain energy is quantitatively successful [3]. If this energy is included in the free energy of the solution, the thermodynamic analysis predicts that the epitaxial lattice-matched alloys are stable at all temperatures, even with the largest likely positive values of the heat of mixing.

Even if the alloys are stable, they will exhibit temperature dependent clustering. A recently published calculation of the equilibrium degree of clustering to be expected [4], does not include the strain energy. Since clustering is accompanied by local density fluctuations and by the strains that result from them, we think that a calculation that omits the strain energy must overestimate the degree of clustering. We have initiated an improved calculation which includes this correction. Such a theory will apply to bulk growth as well as to epitaxy and will be discussed in a future report.

A second experimental finding alluded to above is an extended x-ray absorption fine structure (EXAFS) study of the composition dependence of the anion-cation distances in $Ga_xIn_{1-x}As$ [5]. Since the ionic radii of Ga and In differ by nearly 15%, the lattice parameter is strongly (linearly) dependent on x, changing by 9.3% between the binary end points. Over the same range of composition, however, the anion-cation distances only change by approximately 1.6%. The local structure of tetrahedra consisting of 2 Ga and 2 In atoms surrounding an As atom is very similar to the ionic arrangement in the ordered chalcopyrite structure, and the ionic positions in general are significantly displaced from the sphalerite virtual crystal. Specifically, the lines corresponding to second-neighbor Ga-Ga and In-In distances are broadened, and that of the second-neighbor As-As distance is bimodal.

The implications of these results for our work are twofold. First, they tend to reduce further such confidence as can be placed in calculations of thermodynamic quantities based on the virtual crystal approximation and on the composition dependence of the lattice parameter [1]. At the same time, they raise the speculative possibility that equilibrium epitaxy of an ordered phase may be possible even if the enthalpy of mixing is positive.

The reasoning in support of this statement is as follows: Because of the scatter of cation second nearest neighbor

distances and the two values of anion second nearest neighbor distances in the disordered solid solution, the bond energies cannot all reach their minimum values. Therefore, even if $\varepsilon_{GaIn} - \frac{1}{2}(\varepsilon_{GaGa} + \varepsilon_{InIn}) > 0$ (where ε_{AB} are the interaction energies) for the virtual crystal, this may have little bearing on either the disordered solid solution or on a hypothetical ordered phase, and the uniqueness of the bond distances and energies of an ordered phase may make up for the loss of statistical weight. Moreover, even if the ordered phase is thermodynamically unstable, it will still have a minimum energy configuration which almost certainly will be distorted from the random alloy in symmetry or size or both.

This would offer the possibility of stabilizing an ordered compound by growing on a substrate lattice-matched to the compound but not the solid solution. The substrate would of course be lattice-matched to a different composition of the alloy, with $x \neq 0.5$, but the growth of the alloy could be prevented by control of the melt.

2.2 KINETIC ASPECTS

If long range ordering cannot be made thermodynamically stable, it may still be possible to obtain a degree of order by kinetic effects at the growth surface which are then frozen into the growing crystal.

To achieve such effects, it is necessary to "persuade" each cation species to attach preferentially at one half of

the surface cation sites. This might happen because lattice sites which are equivalent in the bulk may become differentiated in the reduced symmetry of the surface (an obvious crude example of such site differentiation occurs at a growth step). If a growth surface can be found on the sphalerite substrate which separates the surface cation lattice sites into two sublattices that are physically differentiated, then the difference of ionic size and electronegativity between Ga and In may result in a difference in attachment probability. A similar site-preference problem which arises in the growth of a tetrahedral binary compound on an elemental substrate has recently been addressed [6].

In the sphalerite structure, the two lowest-index surfaces on which the fcc ionic lattices divide into two nonequivalent sublattices, are {210} and {211}. In Figure 2.1 we illustrate the principle with a $(1\bar{1}0)$ projection of a $(\bar{1}\bar{1}2)$ surface. The rows of ions that form the surface are drawn with full lines, while the sites where ions are to attach next are shown dashed. The cation sites to be filled next are labeled C1 and C2. The corresponding sites in the interior of the crystal are equivalent, and these sites will become equivalent once the surface has been covered by the new growth. It is apparent, however, that the microscopic topography at sites C1 and C2 is quite different at the point of ionic attachment. It would not be surprising

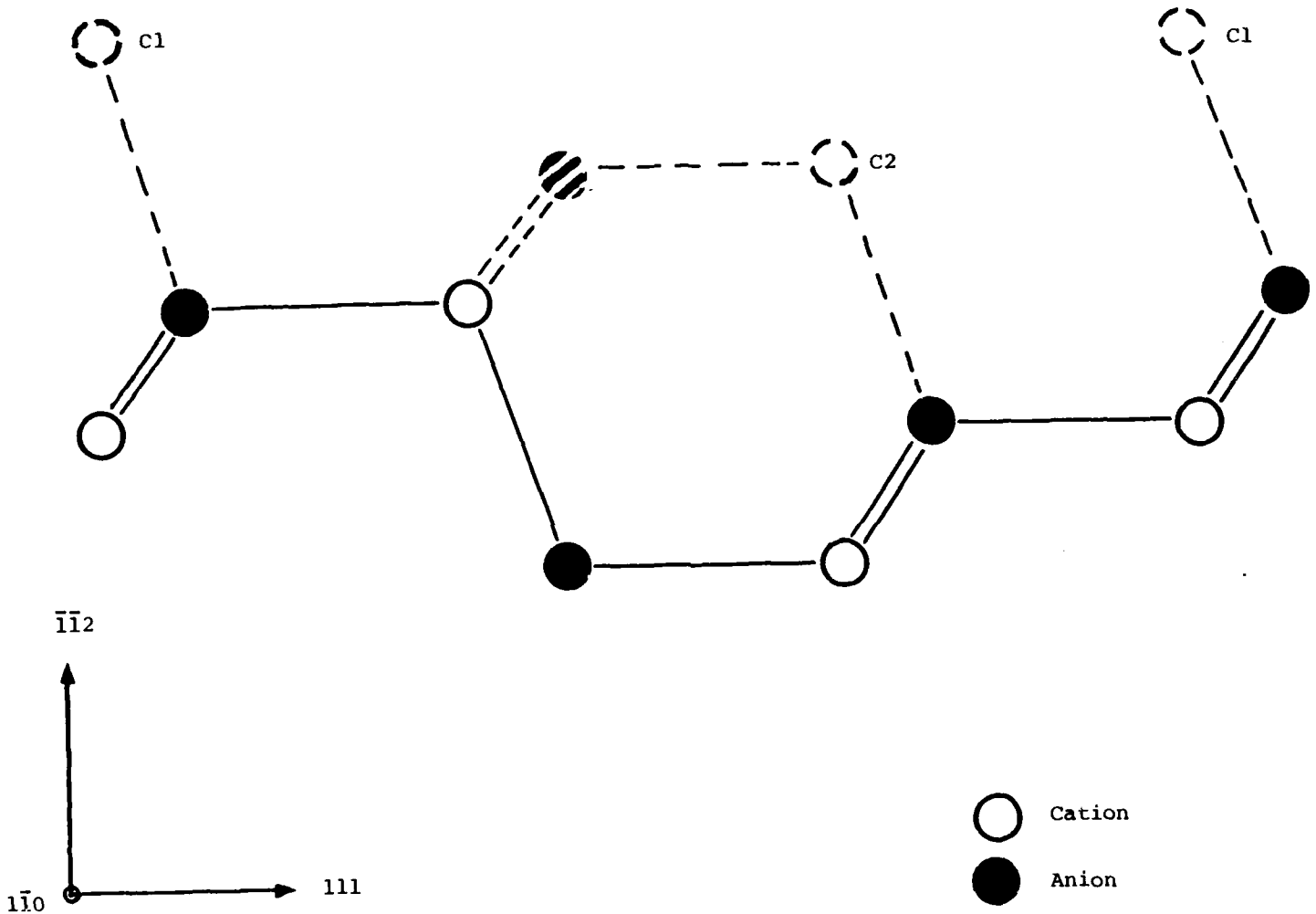

Figure 2.1 $(1\bar{1}0)$ Projection of a sphalerite $(\bar{1}\bar{1}2)$ surface, showing the two non-equivalent cation sites.

if attachment preferences were to be found from a melt containing two species of cation.

An important point to be noted here, to which we shall return presently, is the following: For a given growth surface, such as the $(\bar{1}\bar{1}2)$ shown in Figure 2.1, the surface sublattices do not lose their identity in the course of the growth. In other words, the new non-equivalent sites on the newly formed surface divide into sublattices coherently, in the same way as the underlying atomic plane. Thus, in the extreme case of a growth in which the site preference is complete (in our example, all A cations choosing C1 sites, all B cations choosing C2 sites), the resulting crystal would be fully ordered. Moreover, growth from different nuclei could coalesce coherently, without antiphase boundaries. If the site preference is partial, the ordering may be expected to be partial, but it will nevertheless be long range, with the Bragg-Williams order parameter linearly dependent on the degree of site preference.

The arguments advanced here apply equally to the epitaxy of a ternary compound on a binary substrate, in the sense that a growth face with appropriately lowered symmetry should prevent the occurrence of antiphase boundaries and impose uniqueness of orientation. This view is supported by results on the epitaxy of the chalcopyrite $ZnSnP_2$ on {211} GaAs [7] discussed in Section 3.

We have tacitly assumed in this discussion that the geometry of the exposed growth face is similar to the geometry of the corresponding atomic plane in the interior of the crystal, that is to say, we have neglected surface reconstruction. This assumption is more likely to be a good approximation for a {211} face than for {210}. It has been shown [8] that atomic (hkl) planes for which it is possible to have $h \pm k \pm l = 0$ are neutral (contain equal numbers of anions and cations). If this condition cannot be met, the atomic planes are necessarily charged, giving rise to very large electric fields that must deform the surface.

It has been proposed [9] that the distortion associated with surface reconstruction, and the resulting lowering of the surface symmetry, may be effective in producing ionic site preferences. The idea was supported [9] by favorable results on binary heteropolar epitaxy on an elemental substrate, GaAs on {110} Ge. The {110} Ge surface is thought to relax in a manner which breaks the inversion symmetry and results in some degree of charge transfer between adjacent surface atoms, yielding a strong attachment discrimination between anions and cations. This idea is very plausible and attractive. A possible generalization, in the form of a (2 x 1) reconstruction of a sphalerite surface, might be applicable to our objective, with some reservations. The first of these, which applies to the growth of a stable

compound as well as to the ordering of an alloy by site preference, concerns the size of a reconstruction domain. Unless the domains are fairly large, the epitaxy will have many antiphase boundaries, a point recognized by Kroemer et al [9]. The other difficulty arises only in the growth of an alloy. The propagation of a growth step is known to affect surface reconstruction, and it may well be sufficient to wipe out any site preference. Accordingly we are concentrating on site preferences on surfaces with intrinsically broken symmetry, such as {211}, as described earlier.

2.3 REFERENCES

1. G.B. Stringfellow, J. Appl. Phys. 54, 404 (1983).

2. G.B. Stringfellow, J. Phys. Chem. Solids 33, 665 (1972).

3. G.B. Stringfellow, J. Appl. Phys. 43, 3455 (1972).

4. K.A. Jones, W. Porod, and D.K. Ferry, J. Phys. Chem. Solids 44, 107 (1983).

5. J.C. Mikkelson, Jr. and J.B. Boyce, Phys. Rev. Lett. 49, 1412 (1982).

6. S.L. Wright, M. Inada, and H. Kroemer, J. Vac. Sci. Technol. 21, 534 (1982).

7. G.A. Davis, D. Sc. Thesis, Washington University, 1983.

8. W.A. Harrison, E.A. Kraut, J.R. Waldrop, and W.R. Grant, Phys. Rev. B18, 4402 (1978).

9. H. Kroemer, K.J. Polasko, and S.C. Wright, Appl. Phys. Lett. 36, 763 (1980).

3. $ZnSnP_2$ EPITAXY ON GaAs SUBSTRATES

To examine some of the concepts discussed in Section 2 we have chosen to study chalcopyrite-on-sphalerite growth. $ZnSnP_2$ is an interesting compound for the study of chalcopyrite-on-sphalerite epitaxy due to its lack of tetragonal compression and its close lattice match with the sphalerite GaAs. Such heteroepitaxial systems are also of interest as a potential means of producing high quality chalcopyrite semiconductors and novel heterostructures.

As in sphalerite-on-diamond structure growth [1,2] there are certain difficulties in this heteroepitaxy due to the additional ordering required by the epitaxial material: The idealized GaAs substrate presents a uniform Ga cation sublattice in contrast to the well ordered Zn-Sn cation sublattice of the $ZnSnP_2$. To achieve high quality epitaxy we require that certain Ga sites of the interface be occupied by Zn and the others by Sn to mimic the chalcopyrite structure over the entire growth surface. If this preferential site allocation does not occur, or if it does not mimic the chalcopyrite structure, then the epitaxy will exhibit crystalline defects, such as antiphase domain boundaries, and degraded electrical performance.

We have previously observed these defects in $ZnSnP_2$ grown on {110} and {111} oriented GaAs [3].

In this report we present the results of $ZnSnP_2$ growth experiments performed using {100}, misoriented {110},

and {211} oriented GaAs substrates. These experiments were pursued to determine whether any of these surfaces exhibit the desired preferential site allocation in the context of our growth system. Such allocation may be promoted, for example, by surface reconstruction with charge redistribution or by non-equivalent cation sites in unreconstructed surfaces.

3.1 GROWTH PROCEDURE

The growth procedure used for these experiments was developed and refined during experiments on {110} oriented growth. The details of this procedure are given in [3].

The growth solutions were composed of Zn, Sn, and SnP_3 synthesized in a sealed tube process with a 1.20% equivalent $ZnSnP_2$ concentration in Sn. This provided slightly supersaturated solutions at the homogenization and initial growth temperature of $570.0 \pm 1.0^{\circ}C$, and maintained melt saturation during the two hour homogenization period. Growth was initiated by sliding the solution over the substrate and cooling the system linearly at $3.5 - 4.5^{\circ}C/hr$ for 5 - 16 hours. These conditions produced the optimum growth for all orientations discussed.

The {100} and {211} oriented substrates were prepared as follows: Each as-received wafer was lapped and chemical-mechanical polished using a 4% $Br-CH_3OH$ solution so both surfaces were uniform and free of gross damage. Such damage was usually evident after a 20 second etch in the

Br-CH_3OH solution. After scribing and breaking each wafer into substrates of the proper dimensions for the LPE boat the substrates were cleaned in boiling trichloroethylene, acetone, and methyl alcohol. Each substrate was etched for 2 minutes in a 10:1:1 H_2SO_4:H_2O_2:H_2O solution 10 minutes after initial mixing and rinsed thoroughly in DI H_2O just prior to loading.

The misoriented {110} substrates were prepared individually after scribing and breaking the wafers into the proper sized pieces. Each substrate was mounted on a 2° angle lapping block and lapped and polished as above. The substrate was then remounted face down on a 0° lapping block and the lapping and polishing procedure was repeated. The resultant substrates had parallel polished faces at an angle of $2.0 \pm 0.2°$ from the initial {110} surfaces. These substrates were subsequently cleaned and etched as outlined above.

In this work the misorientation in two orthogonal direction was examined: misorientation towards a perpendicular <110> direction and towards a perpendicular <001> direction. The direction of misorientation was determined from the perpendicular cleavage planes of the wafers: those misoriented towards a perpendicular cleavage plane are misoriented towards a perpendicular <110> direction; those misoriented along a perpendicular cleavage plane

are misoriented towards a perpendicular <001> direction. For brevity these orientations will be denoted as the {110}/<110> and {110}/<001> orientations, respectively.

3.2 LAYER MORPHOLOGY

Typical layers grown using these growth procedures are shown in Figures 3.1 to 3.4. $ZnSnP_2$ growth on {100} oriented GaAs showed no improvement over our initial growth experiments. These layers had smooth interfaces but rough surfaces containing numerous pits which often extended to the interface. This morphology is reminiscent of lattice matched $Zn_xCd_{1-x}SnP_2$ ($x = .125$) growth on {100} oriented InP [4]. Because of the gross pitting these layers were not examined further. Growth on the {100} orientation is of interest since most chalcopyrite-on-sphalerite epitaxy is performed using this orientation.

Typical $ZnSnP_2$ growth on the {110}/<001> orientation is shown in Figure 3.1. These layers are 5-7μm thick for a 16 hour growth time with very smooth interfaces and moderately smooth surfaces exhibiting some faceting. This growth is quite similar to that achieved on the nominal {110} orientation with the exception of the increased faceting.

Growth on the {110}/<110> orientation showed marked improvement over growth on the {110} and {110}/<001> orientations. A typical $ZnSnP_2$ layer grown on this

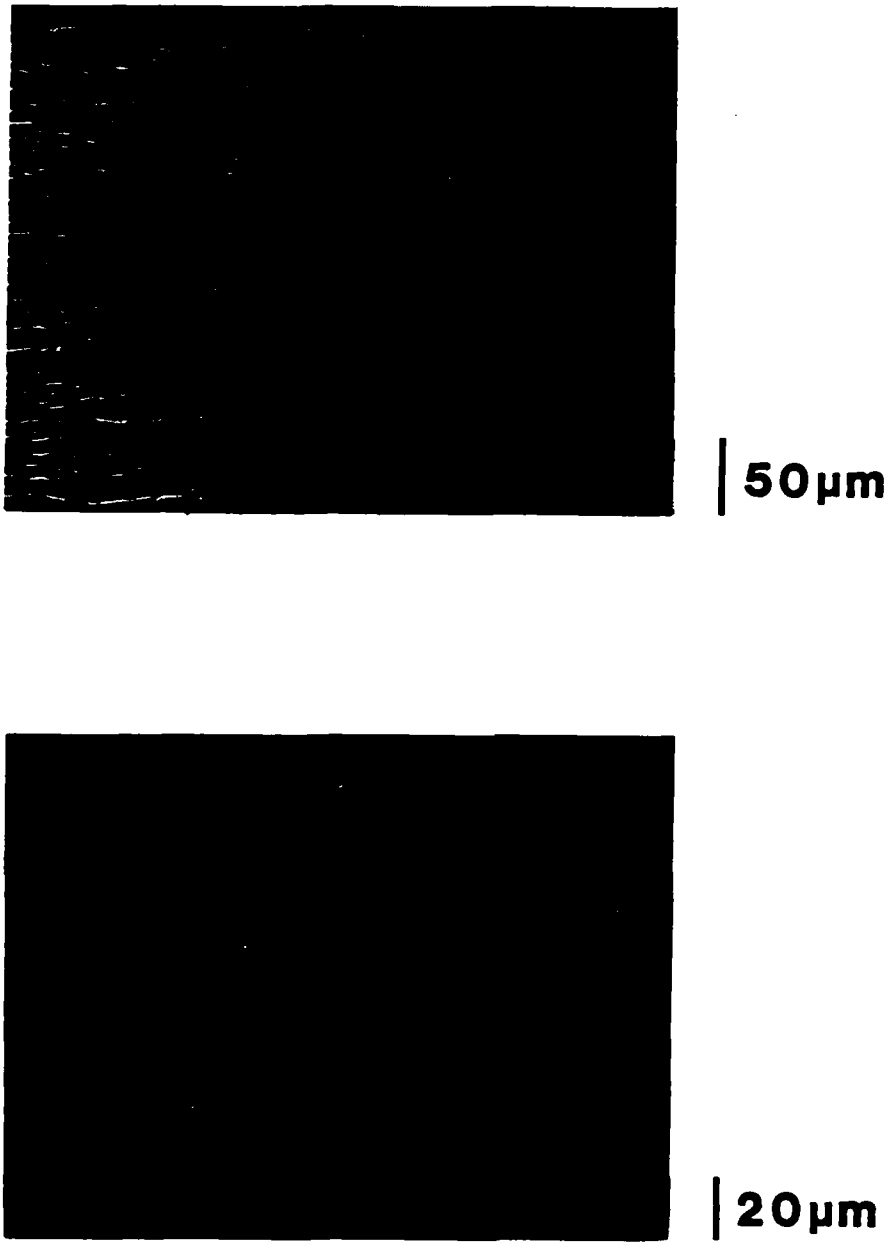

Figure 3.1 Surface and cross-sectional views of $ZnSnP_2$ grown on GaAs misoriented 2° off the {110} towards a perpendicular <100>.

orientation is shown in Figure 3.2. These layers are 20-25μm thick for a 16 hour growth time with smooth interfaces and surfaces. This growth exhibits much less surface faceting than {110} and {110}/<001> growth.

$ZnSnP_2$ layers grown on {211}As and {211}Ga oriented GaAs are shown in Figures 3.3 and 3.4, respectively. Growth on the {211}As orientation is 20-25μm thick for a 16 hour growth time with smooth interfaces and fairly smooth surfaces containing some growth facets. The {211}Ga orientation growth is similarly 20-25μm thick for a 16 hour growth time with smooth interfaces and surfaces exhibiting minimal faceting. It is interesting to note that the cross-sectional view of Figure 3.4 shows no rippling observed in the other cross sectional view suggesting this growth has improved crystallinity. While this growth is the most sensitive to changes in the growth conditions, it can be reproducibly obtained.

3.3 TETRAGONAL AXIS ORIENTATION

To examine the structure of the epitaxial $ZnSnP_2$ and determine the relative orientations of the tetragonal axis of the chalcopyrite layer with respect to the cubic axes of the sphalerite substrate, back reflection Laue photographs were taken. A determination of the tetragonal axis orientation relative to the cubic axes is fundamental to this work since the existence of only one relative orientation is a necessary (but not sufficient) condition for

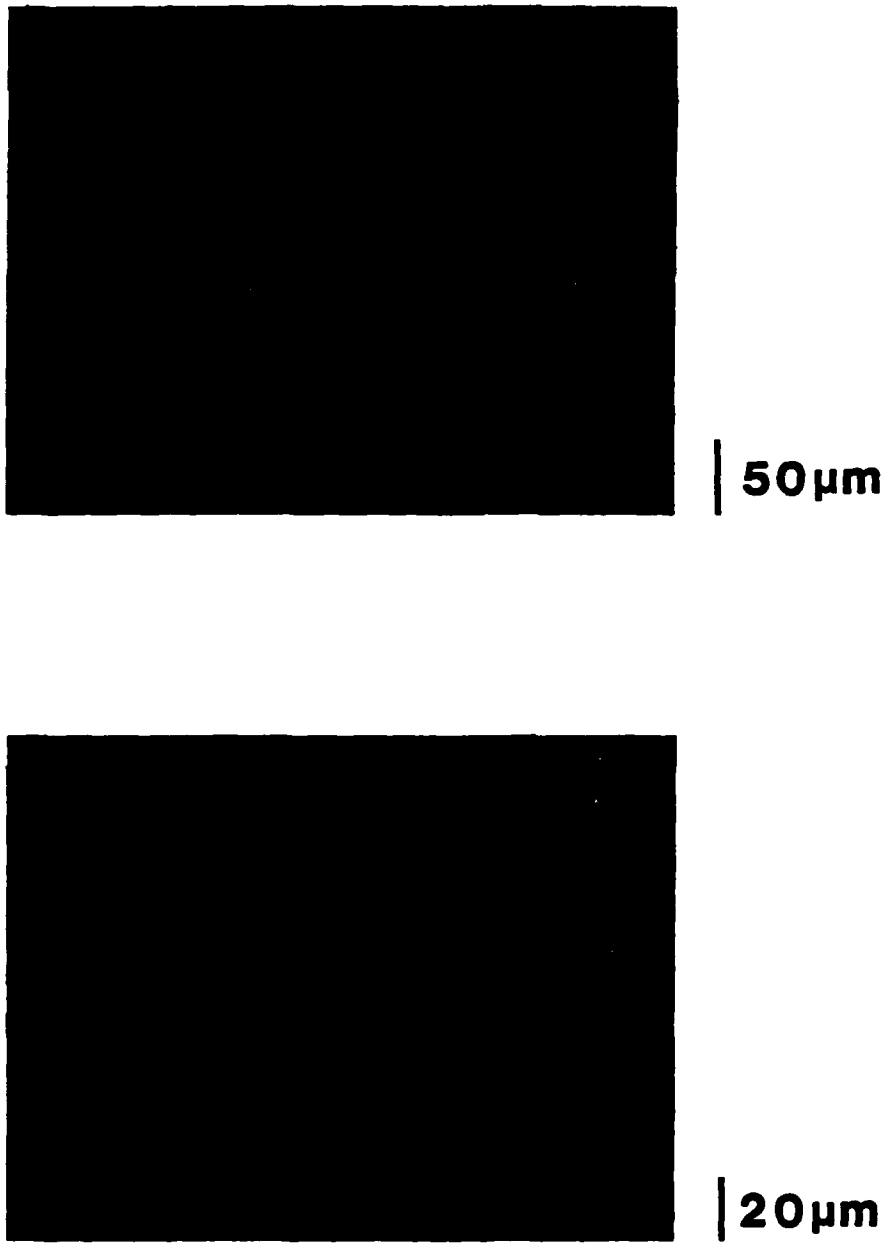

Figure 3.2 Surface and cross-sectional views of $ZnSnP_2$ grown on GaAs misoriented 2° off the {110} towards a perpendicular <110>.

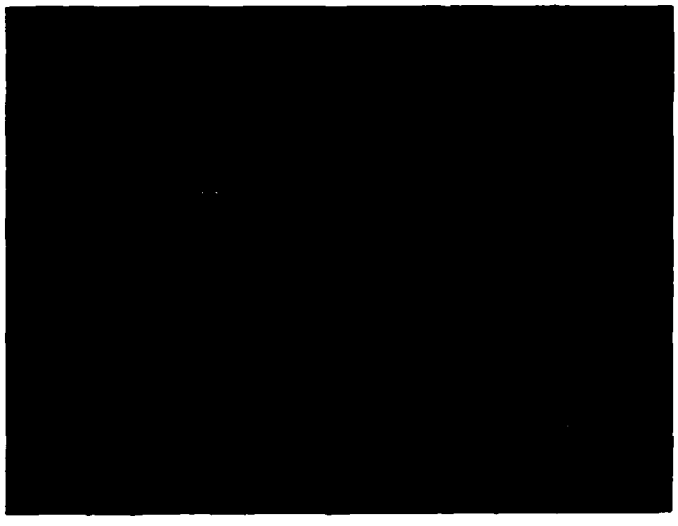

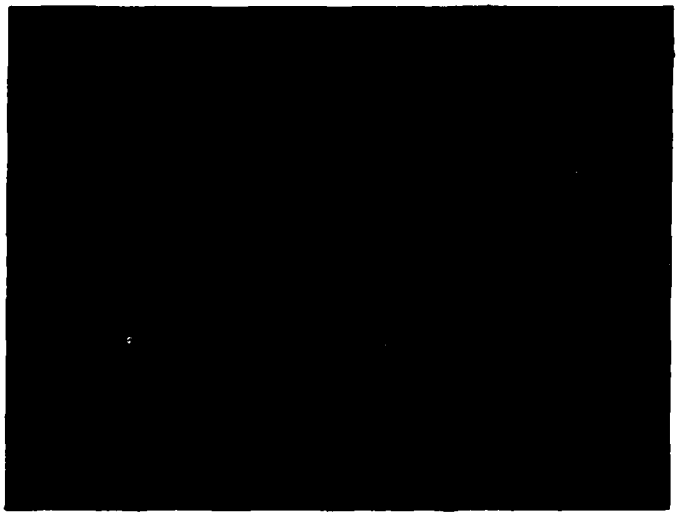

Figure 3.3 Surface and cross-sectional views of $ZnSnP_2$ grown on {211}As GaAs.

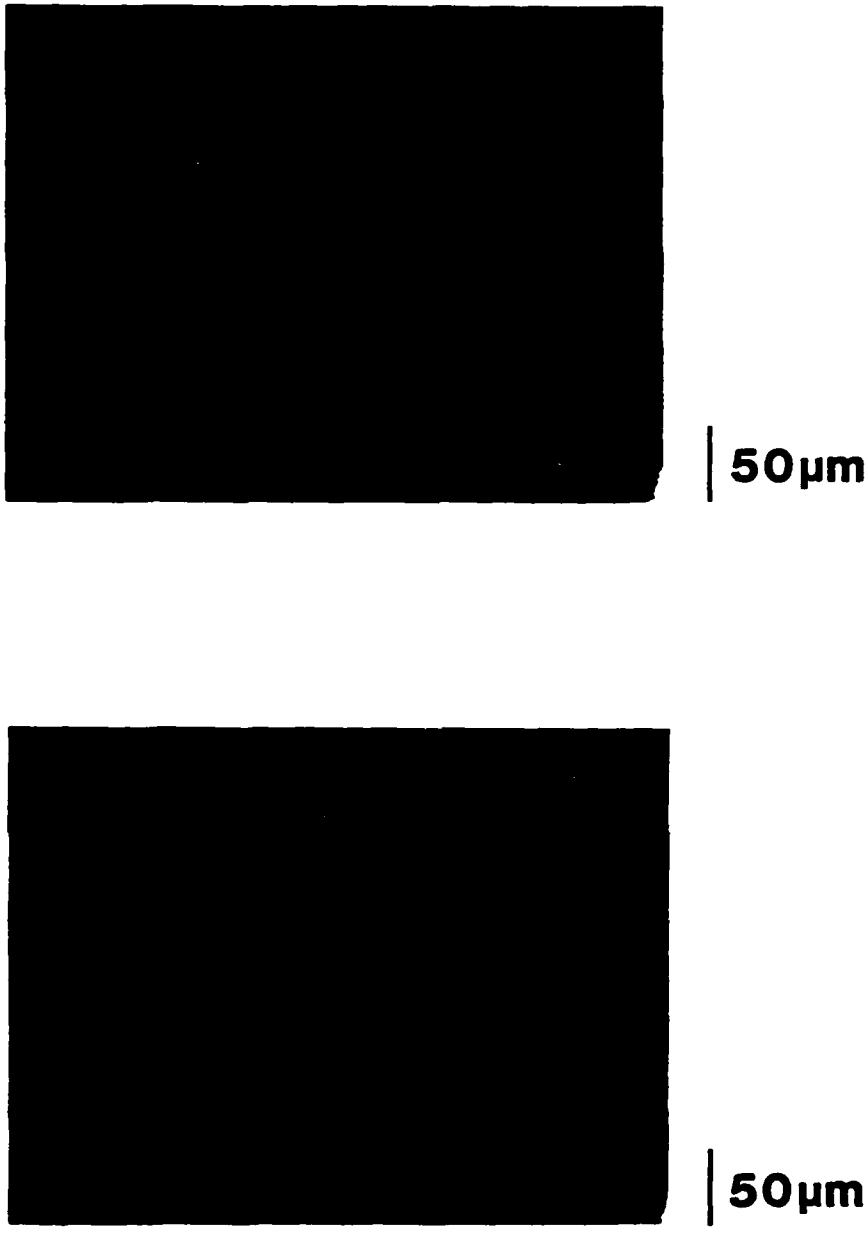

Figure 3.4 Surface and cross-sectional views of $ZnSnP_2$ grown on {211}Ga GaAs.

defect-free growth. The technique used was adapted from our previous observations of allowed reflections from the chalcopyrite structure for {110} oriented growth [3].

The experimental arrangement for the photographs is illustrated schematically in Figure 3.5. In all Laue photographs the heterostructures were oriented so the Cu x-rays were incident along one of the <110> directions of the substrate. If the epitaxy is oriented so that this corresponds to a <021> chalcopyrite direction, then four additional diffracted spots - the 259, 167, $\bar{2}59$, and $\bar{1}67$ diffractions - will be evident in the photographs.

It can be seen from Figure 3.5 that the particular orientation shown will produce these four additional spots on one side of the photograph. If the chalcopyrite were oriented with its tetragonal axis along the [010] axis of Figure 3.5 then the reflections would be observed on the other side of the film. Thus, with one such Laue photograph we observed whether two of the three possible relative orientations of the tetragonal axis (c-axis) are present in the epitaxy. The third possible relative orientation of the c-axis can be observed by using a different <110> direction as the primary direction. For the case of Figure 3.5 one could observe chalcopyrite growth oriented with the tetragonal axis along the [100] axis in Laue photographs made using the [110] or [101] direction as the primary direction.

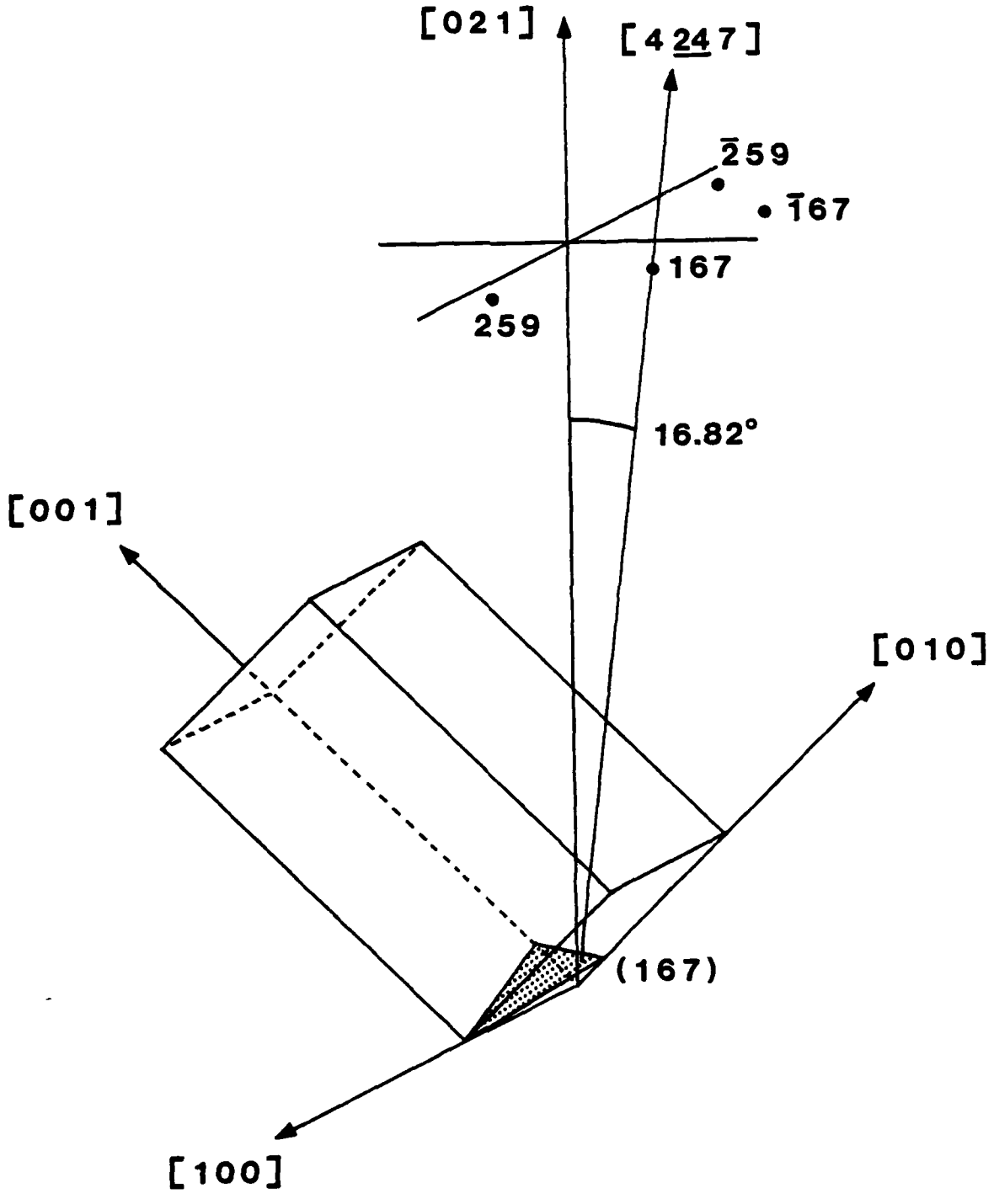

Figure 3.5 Schematic of allowed chalcopyrite reflections.

Some typical Laue photographs are shown in Figures 3.6, 3.7, and 3.8. Figure 3.6 is a photograph taken of a layer grown on (112) oriented GaAs with the [101] direction as the primary direction. This photograph clearly shows the four asymmetric chalcopyrite spots observed when only one relative orientation is present. Figure 3.7 is a photograph of a layer grown on {110}/<110> oriented GaAs. The primary direction for this photograph was the [110] axis 2° off the surface normal. This photograph contains four high intensity chalcopyrite spots associated with one relative orientation as well as four low intensity chalcopyrite spots (opposite the former spots) associated with a less abundant second relative orientation of the c-axis. Figure 3.8 is a photograph of a layer grown on nominal {110} oriented GaAs which reveals eight uniform chalcopyrite spots. This photograph was taken with the surface normal as the primary direction and indicates that this epitaxy contains equal amounts of two relative orientations of the c-axis.

The relative orientations observed for $ZnSnP_2$ grown on the various GaAs substrates are illustrated schematically in Figures 3.9 to 3.12. In these figures the shaded planes indicate the growth surfaces and the arrows along the principal axes of the cubic sphalerite structure indicate the relative abundance of the three possible chalcopyrite

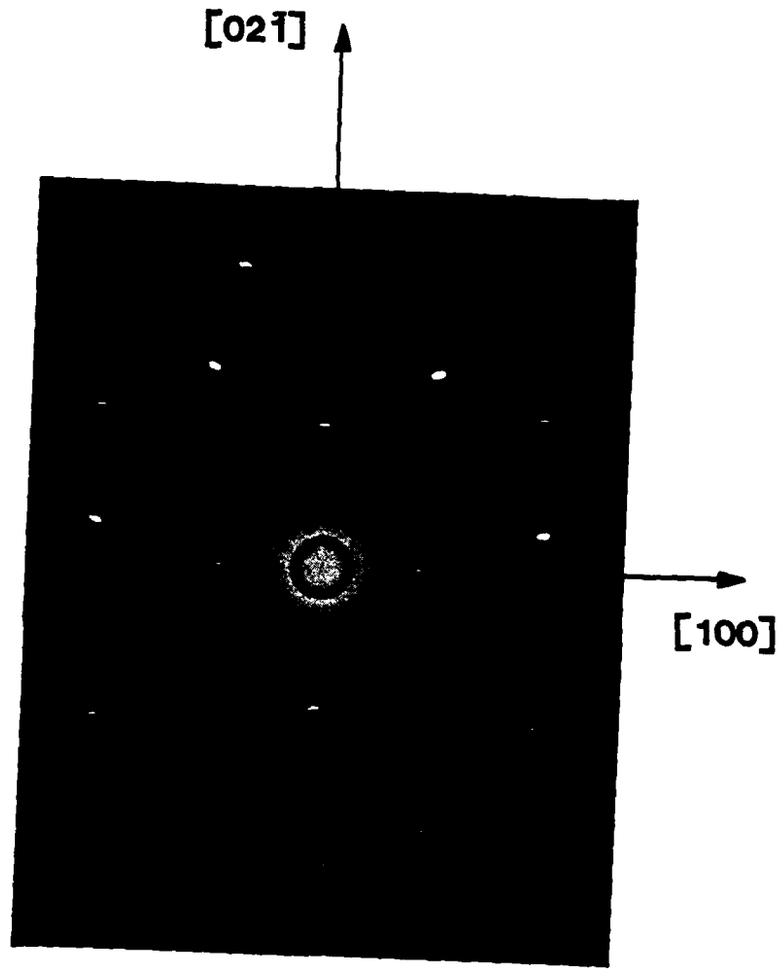

Figure 3.6 Laue photograph of $ZnSnP_2$ grown on (112)GaAs with primary x-ray beam in [101] direction.

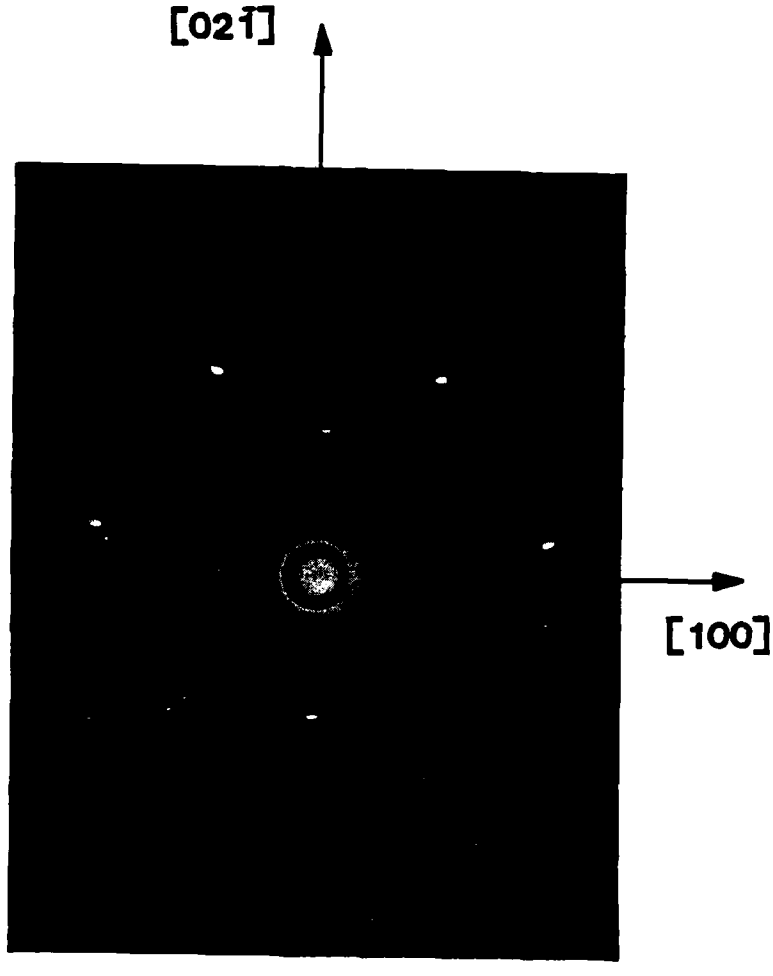

Figure 3.7 Laue photograph of $ZnSnP_2$ grown on {110}/<110> GaAs with primary x-ray beam in [110] direction 2° off the surface normal.

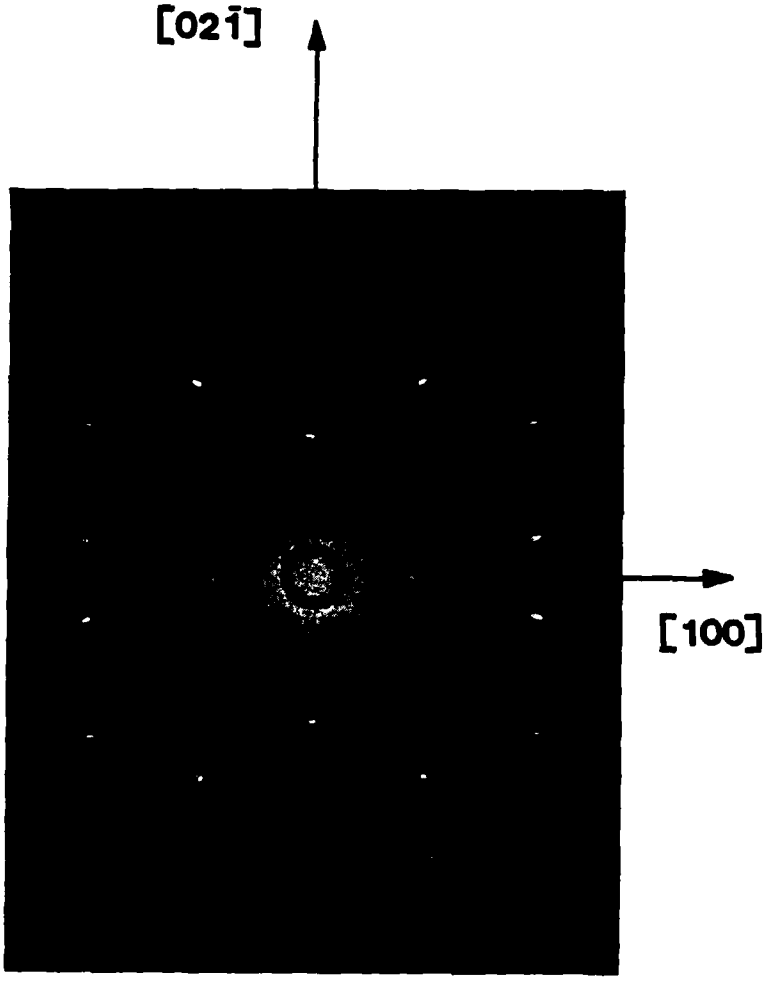

Figure 3.8 Laue photograph of $ZnSnP_2$ grown on nominal {110} GaAs with primary x-ray beam along surface normal.

orientations. The arrows are denoted $[001]_c$ to indicate the chalcopyrite tetragonal axis. The lengths of the arrows illustrate the relative abundance of each orientation.

Figure 3.9 illustrates the relative orientations observed previously in {110} orientation growth [3]. In such growth the epitaxy contained equal amounts of material oriented with its tetragonal axis along the [100] and [010] axes and no material oriented with its tetragonal axis along the [001] axis.

The peculiar nature of this growth was the impetus behind the misorientation experiments. A possible explanation for this growth habit is the reconstruction of the GaAs cation sublattice in the {110} surface into alternating Zn-like and Sn-like rows extending in the [001] direction. This arrangement does not mimic the chalcopyrite structure (alternating double rows on Zn and Sn atoms for the (021) surface) and is expected to produce layers with antiphase boundaries. By misorienting off the {100} surface it may be possible to produce a surface which better mimics the chalcopyrite structure and results in improved growth.

Laue photographs of {110}/<001> orientation growth showed no detectable difference from those of nominal {110} growth. Photographs of {110}/<110> growth, however, reveal an improved growth habit as illustrated in Figure 3.10. Growth on this orientation revealed a significant

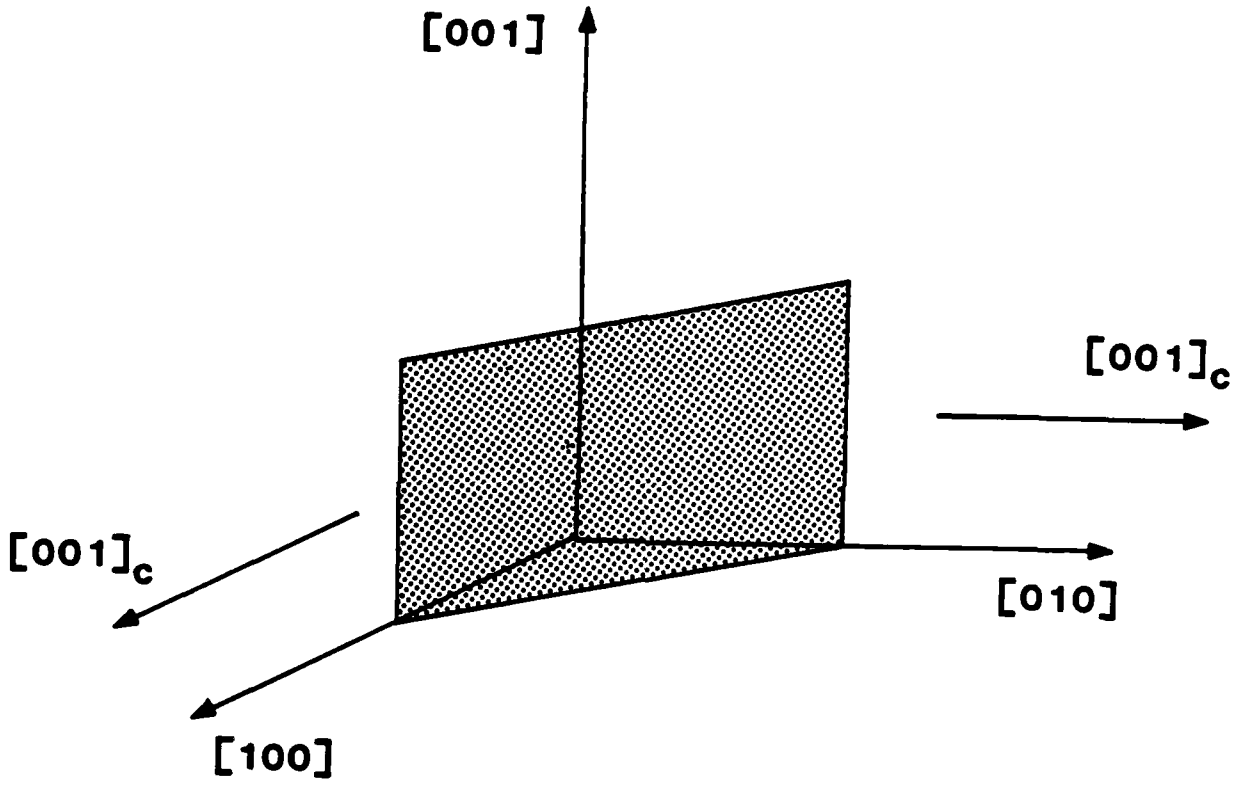

Figure 3.9 Schematic illustration of the observed relative orientations of $ZnSnP_2$ grown on {110} GaAs.

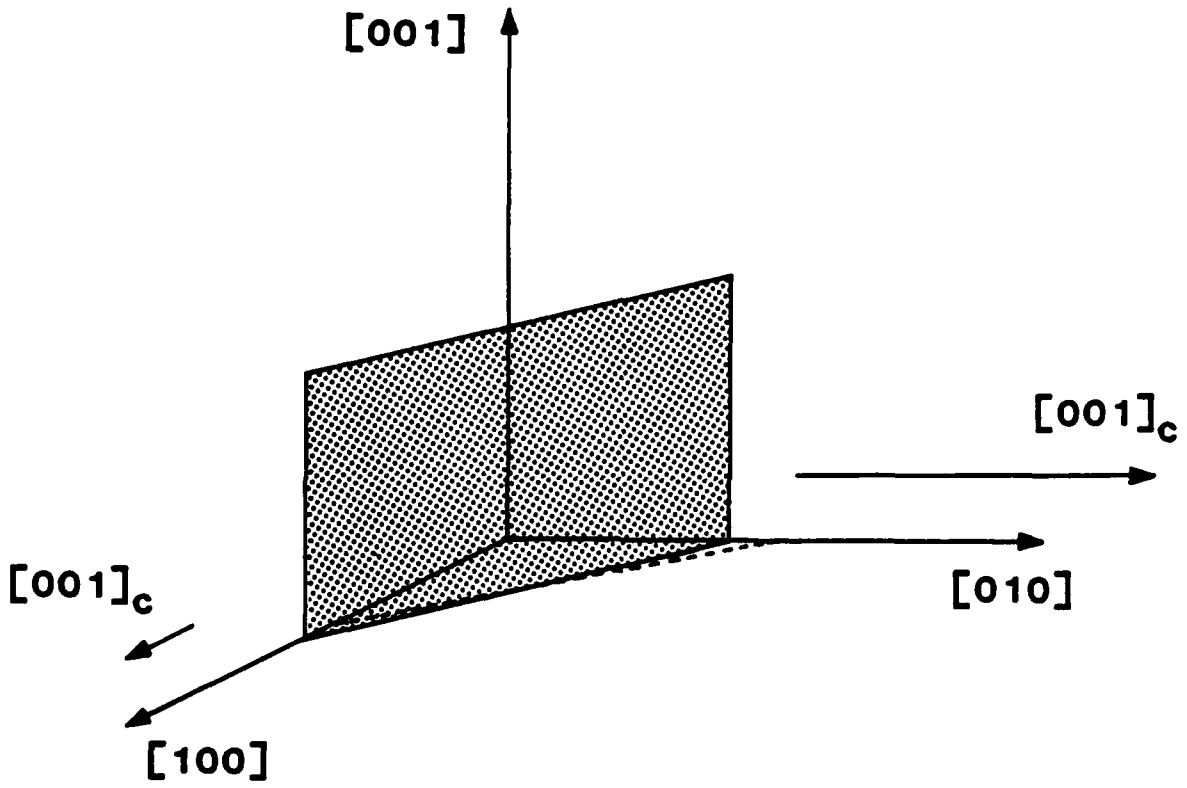

Figure 3.10 Schematic illustration of the relative orientations of $ZnSnP_2$ grown on {110}GaAs misoriented 2° towards a perpendicular <110>.

increase in the abundance of material oriented with its tetragonal axis along the [010] direction and a decrease of the other relative c-axis orientation. In some layers grown on this orientation the smaller relative c-axis orientation was not observed. Variations in the relative abundance of the two relative orientations may be due to unintentional misorientation of the substrates during preparation.

Laue photographs of {100} oriented growth indicate that all three possible orientations are present as illustrated in Figure 3.11. This suggests that the {100} orientation may be the least favored orientation for chalcopyrite-on-sphalerite systems [5].

The {211}As and {211}Ga growth revealed the best results in that only one relative orientation was observed. This is illustrated in Figure 3.12 which shows the observed relative orientation of the tetragonal axis along the [001] direction for a (112) surface. This habit was observed in all {211} growth, regardless of morphology, indicating that this orientation may be the best for high quality epitaxy.

3.4 RESISTIVITY AND HALL MEASUREMENTS

Van der Pauw resistivity and Hall measurements made on the $ZnSnP_2$ layers show improved electrical characteristics associated with the suppression of antiphase boundaries. The layers grown on {110} and {110}/<001> substrates were

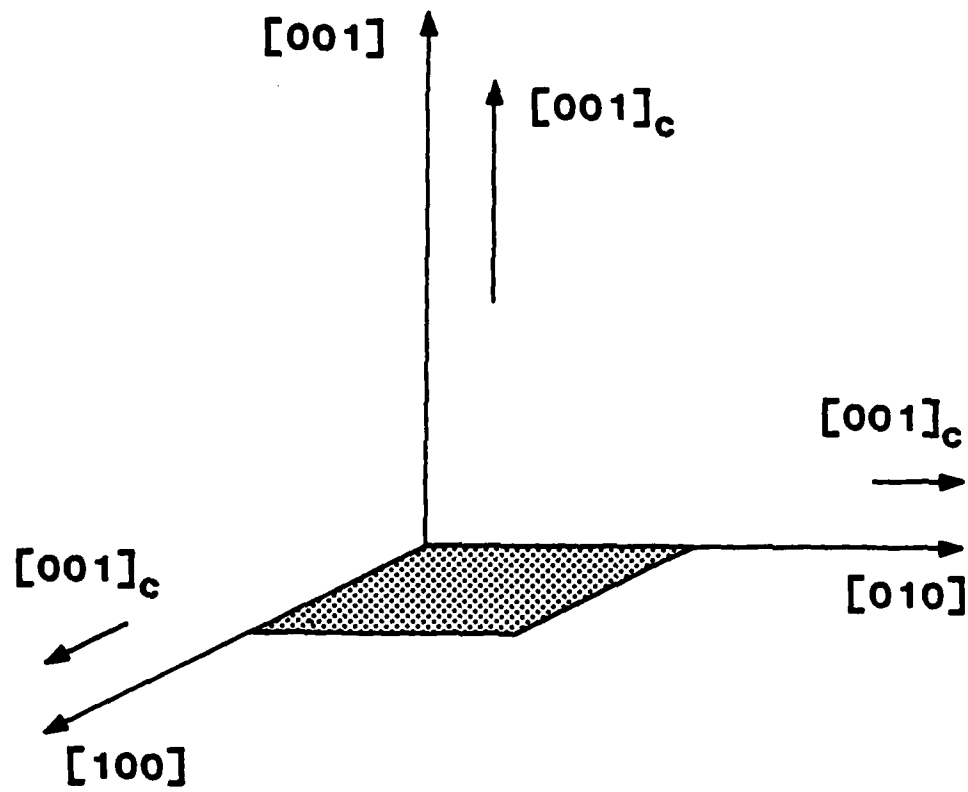

Figure 3.11 Schematic illustration of the relative orientations of $ZnSnP_2$ grown on {100} GaAs.

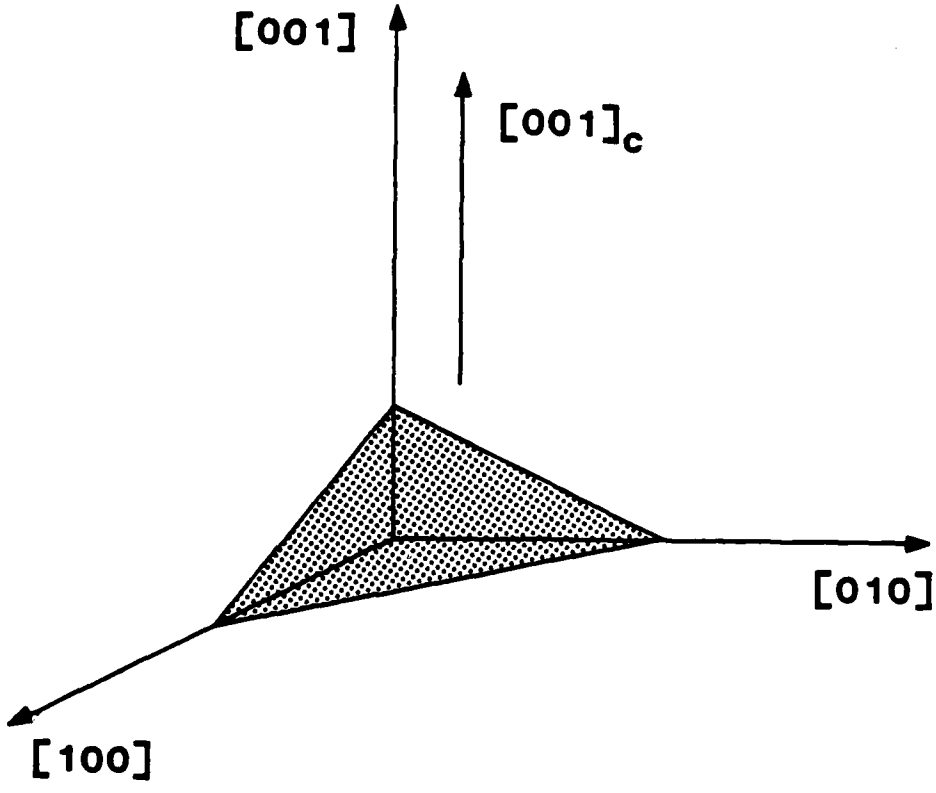

Figure 3.12 Schematic illustration of the relative orientation of $ZnSnP_2$ grown on {211} GaAs.

p-type with carrier concentrations of 3-5x10^{19}cm^{-3} and calculated mobilities of 15-40cm^2/V sec. $ZnSnP_2$ layers grown on {110}/<110> oriented GaAs, which had improved crystallinity associated with the suppression of a second relative c-axis orientation, had p-type carrier concentrations of 2-5x10^{18}cm^{-3} and mobilities of 20-45cm^2/V sec. $ZnSnP_2$ grown on {211} oriented GaAs, which had only one c-axis, had carrier concentrations and mobilities similar to the {110}/<110> layers.

3.5 COMPOSITIONAL ANALYSIS

To determine the composition of the epitaxial layers, electron microprobe analysis was performed. All layers grown on {100}, {110}, and {211} GaAs substrates were determined to be very nearly stoichiometric $ZnSnP_2$. The analysis indicated a slight tendency to incorporate Ga into the layers near the interface with the Ga level being less than one molar percent. No As was found in any of these layers. The layers grown on {111} GaAs substrates, however, were determined to be alloys of GaP and $ZnSnP_2$.

These layers were approximately 12% GaP for a 570°C initial growth temperature and primarily GaP for a 630°C initial growth temperature. The later layers were very poor in crystal quality. The source of the Ga is presumably etching of the GaAs substrates prior to growth. The {111} layers typically have rough interfaces indicating that there is etch-back prior to growth. No As was

observed in these layers which indicates that the segregation coefficient for As is very small compared to that for Ga.

3.6 PHOTOCONDUCTIVITY MEASUREMENTS

To determine the bandgap of the epitaxial $ZnSnP_2$, photoconductivity measurements were made. Results of some of these measurements are shown in Figures 3.13 and 3.14. The values of bandgaps were determined from the data by differential analysis. Figure 3.13 shows the response from a {211}Ga layer. This scan reveals a bandgap of 1.39eV associated with the GaAs substrate and a bandgap of 1.45eV associated with the $ZnSnP_2$ epitaxy. The 1.45eV value is smaller than the 1.66eV value previously reported [6]. The scan in Figure 3.14 was taken from a {111}As grown layer which was determined to be 12% GaP from microprobe analysis (a Laue photograph indicated that this layer was sphalerite). This scan shows a transition at 1.39eV again associated with the GaAs substrate but also one at slightly higher energy ($\simeq$1.40eV) associated with the layer. This is of interest since it reveals a decrease in the bandgap from values of 1.45eV for $ZnSnP_2$ and 2.24eV for GaP. This is contrary to the behavior predicted by the conventional virtual-crystal model which predicts a monotonic variation in band-gap with alloy composition.

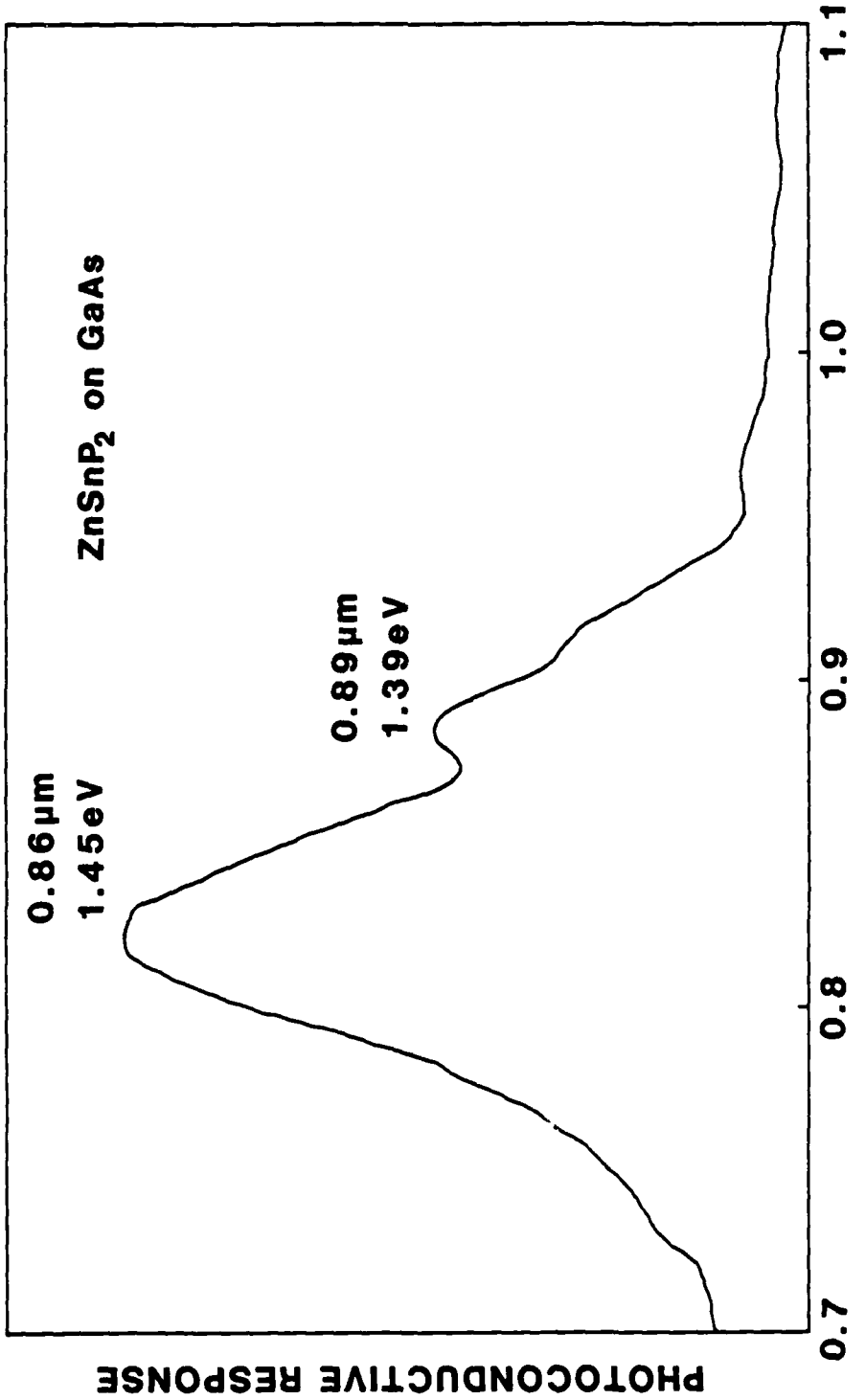

Figure 3.13 Photoconductive response of a $ZnSnP_2$ layer grown on {211} Ga oriented GaAs.

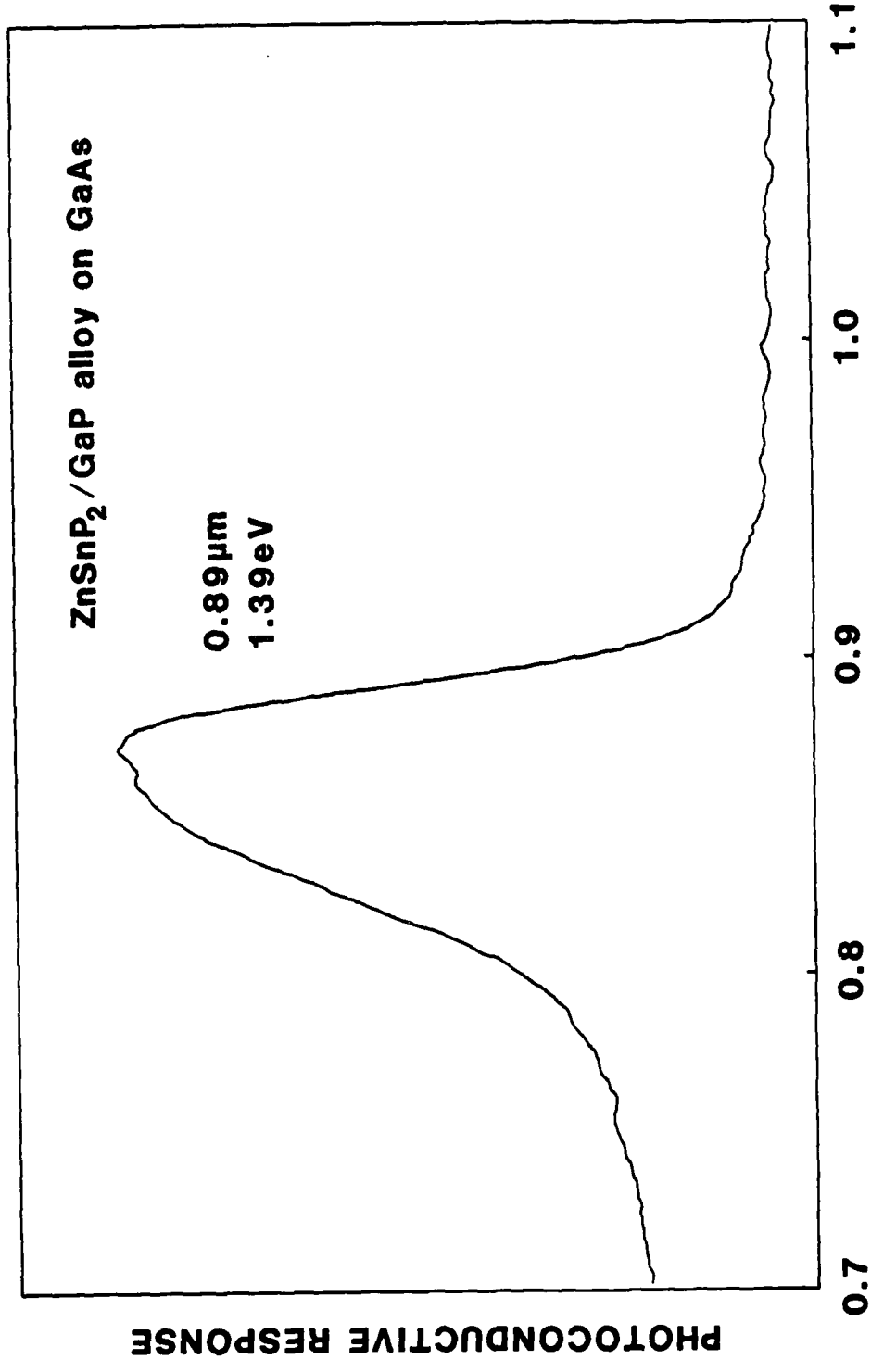

Figure 3.14 Photoconductive response of a $(GaP)_{0.12}(ZnSnP_2)_{0.94}$ layer grown on {111} As oriented GaAs.

Such behavior has been observed in metastable alloys of Ge and GaAs [7] where it is attributed to a phase transition from sphalerite to diamond phases. An analogous explanation for the $(GaP)_{2x}(ZnSnP_2)_{1-x}$ system seems likely: a lowering of the bandgap is observed for $x \approx 0.06$ in conjunction with a phase transition from chalcopyrite to sphalerite phases. The {111} growth provides an easy means for investigating this behavior since the alloy composition can be varied by changing the initial growth temperature. Such an investigation may be a subject for future study. The predicted dependence of bandgap on alloy composition is suggested in Figure 3.15.

3.7 REFERENCES

1. H.Kroemer, K.J. Polasko, and S.C. Wright, Appl. Phys. Lett. 36, 763 (1980).

2. S.L. Wright, M. Inada, and H. Kroemer, J. Vac. Sci. Technol. 21, 534 (1982).

3. G.A. Davis and C.M. Wolfe, J. Electrochem. Soc. 130, 1408 (1983).

4. G.A. Davis and C.M. Wolfe, J. Electronic Mat. 11, 505 (1982).

5. J.E. Andrews, H.H. Stadelmaier, M.A. Littlejohn, and J. Comas, J. Electrochem. Soc. 128, 1563 (1981).

6. J.L. Shay and J.H. Wernick, Ternary Chalcopyrite Semiconductors (Pergamon Press, Oxford, 1975).

7. Kathie E. Newman and J.D. Dow, Phys. Rev. B 27, 7495 (1983).

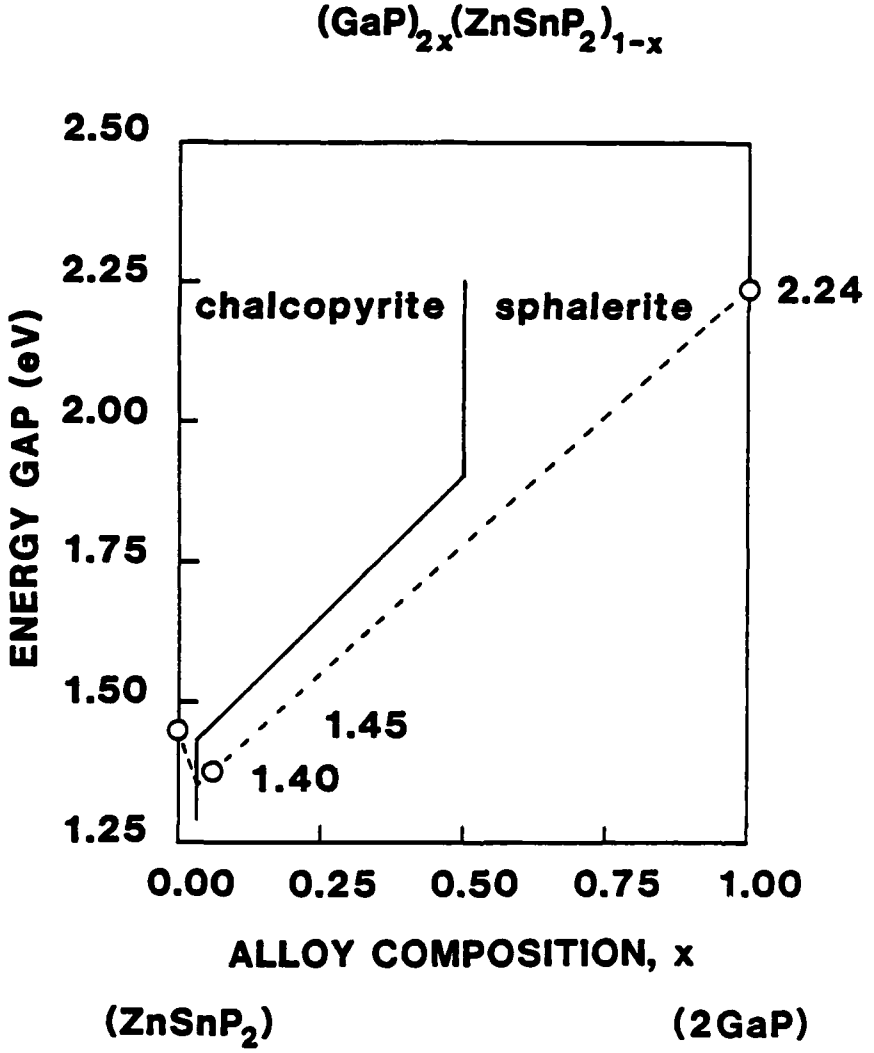

Figure 3.15 Possible behavior of energy gap as a function of alloy composition for $(GaP)_{2x}(ZnSnP_2)_{1-x}$ alloys.

4. $Ga_xIn_{1-x}P$ EPITAXY ON GaAs SUBSTRATES

To examine the conclusions of the previous sections we are examining conditions for the growth of $Ga_xIn_{1-x}P$ on different GaAs substrate orientations.

4.1 GROWTH PROCEDURE

The apparatus used for the liquid phase epitaxial (LPE) growth of $Ga_xIn_{1-x}P$ consists of a horizontal furnace system with a conventional sliding boat machined from high purity graphite. Pd diffused high purity hydrogen flows through a silica tube. The growth temperature is monitored by a thermocouple mounted in the furnace near the silica tube.

Semi-insulating Cr doped {100}, {110}, {111}, and {211} oriented GaAs wafers are prepared for growth by lapping to remove saw damage and polishing with 1% bromine in methyl alcohol. These substrates are then cut in 6.3mm x 6.3mm pieces and degreased by boiling successively in trichloroethylene, acetone, and methyl alcohol. Prior to insertion of a substrate into the boat, a chemical etch in $10H_2SO_4$: $1H_2O_2$:$1H_2O$ is performed. The melt is prepared by adding weighted amounts of InP and GaP to 1.2 gms of In, corresponding to a solution height of 4mm. After the growth melt and substrate are loaded into the boat the system is purged with hydrogen to remove oxygen and water vapor.

The source melt is heated for 1 hour at 10°C above the saturation temperature to ensure that the components

are completely melted. The melt temperature is then lowered to the growth temperature. After the furnace temperature is stabilized, the melt is then brought onto the substrate and constant temperature is maintained until the desired growth time is completed. Upon completion of growth, the melt is wiped off by the slider, and the boat is rapidly cooled to room temperature. Any residual melt is removed from the surface with a solution of mercuric chloride in dimethyl formamide.

A number of studies of the In-Ga-P ternary phase diagram have been reported in the literature [1-9]. The initial liquidus compositions used for our growth experiments were obtained from Stringfellow et al. [5], Ohta et al. [6], Lewis [7], and Hitchens et al. [10]. LPE growth of $Ga_xIn_{1-x}P$ on {100}, {110}, and {111}As GaAs substrates was performed using the step cooling method described in these papers with little success. In all grown layers substrate surfaces were etched back and melt inclusions were observed as shown in Figure 4.1. The surfaces were usually rough and heavily covered with melt. Because of this, an additional layer was usually grown from the melt left on the surface when the boat was rapidly cooled to room temperature.

In an attempt to obtain lattice matched growth and improved morphology, the published melt compositions were

Figure 4.1 Typical layer grown with published liquidus data shows substrate etch-back and melt inclusions.

adjusted by trial and error at the same growth temperature as above. In this manner, we were able to grow some layers with flat interface but rough surfaces. However, these results were not reproducible. This failure to obtain good lattice matched growth by the step cooling method using published liquidus data is probably due to kinetic effects which vary from one LPE reactor to another. Thus, it was necessary to determine liquidus data for our reactor by the following growth technique. First it is known [11] that the free energy of pure InP is always higher than the solid alloy which is in equilibrium with an In-Ga-P melt, while a GaP substrate is stable. When a mixture of In-InP-GaP is heated to a high temperature, the InP crystal dissolves in the In-solution completely [4,11] and automatically determines the solubility of GaP. We can, therefore, easily control the equilibrium composition of the liquid solution by adding a weighted amount of InP and an excess amount of GaP. The quantity of InP added to 1.2 g of In metal was varied, so that the melt would be properly supersaturated to suppress melt back of the substrate surface and yield lattice-matched growth. For convenience, a cooling rate of 0.5°C/min was used during the growth period. Constant temperature growth can be performed once the liquidus data and the degree of supersaturation needed for growth are known.

4.2 ORIENTATION DEPENDENCE

Using this procedure lattice matched $Ga_xIn_{1-x}P$ was easily grown on {111}As and {110} GaAs substrates. Table 4.1 shows liquidus and solidus data for $Ga_xIn_{1-x}P$ layers grown on {110} GaAs substrates. Cross sections of layers grown on {110} substrates were typically characterized by a rough surface and a flat interface, as shown in Figure 4.2. X-ray diffraction measurements were employed to analyze the composition of the grown materials by using a double crystal diffractometer aligned for the GaAs 333 reflection with Cu Kα radiation. X-ray analysis of {110} oriented samples showed a single broadened GaAs peak as shown in Figure 4.3. The full widths at half maximum (FWHM) peak widths ranged from 82 to 95 seconds, indicating that all of these layers lattice-matched the GaAs substrates with relative ease.

Table 4.2 shows liquidus and solidus data for layers grown on {111}As substrates. Cross sections of samples grown on {111}As substrates were characterized by a relatively smooth surface and a flat interface, as shown in Figure 4.4. The typical layer thicknesses were 1 to 3 μm. The substrate surface suffered no meltback and no source melt was left on the surface. Some pitting of the GaAs surface, however, was observed. This is apparently due to an interaction of the surface with phosphorus lost from the melt [12]. To circumvent this problem, the GaAs substrate

Table 4.1 Data for $Ga_xIn_{1-x}P$ layers grown on {110} GaAs.

Run	X^l_{In}	X^l_{Ga}	X^l_P	$W^{(g)}_{InP}$	$T^{(°C)}_{growth}$	X^s_{Ga}
78	0.9375	0.0190	0.044	0.0418	796-790	--
68	0.9454	0.0146	0.040	0.0421	799-790	0.52
77	0.9375	0.0185	0.044	0.0426	799-790	--
70	0.9380	0.0180	0.044	0.0434	799-790	0.52
66	0.9464	0.0136	0.040	0.0437	799-789	0.52
76	0.9385	0.0175	0.044	0.0442	797-794	--
73	0.9390	0.0170	0.044	0.0451	799-790	0.52
69	0.9474	0.0126	0.040	0.0453	799-790	--

Figure 4.2 Typical layer grown on {110} GaAs substrate.

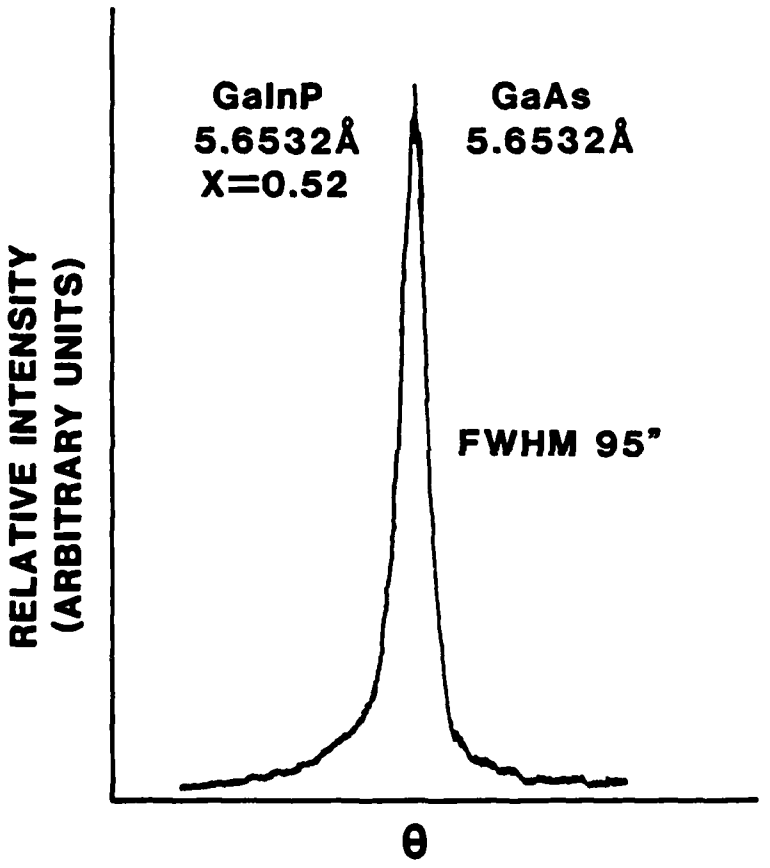

Figure 4.3 X-ray scan of {110} sample.

Table 4.2 Data for $Ga_xIn_{1-x}P$ layers grown on {111} As GaAs.

Run	X^l_{In}	X^l_{Ga}	X^l_P	$W^{(g)}_{InP}$	$T^{(°C)}_{growth}$	X^s_{Ga}	
80	0.952	0.011	0.037	0.0428	799-790	0.52	0.44
82	0.952	0.010	0.037	0.0428	794	--	--
95	0.938	0.018	0.044	0.0434	799-790	--	--
97	0.938	0.018	0.044	0.0434	799-789	0.51	0.45
85	0.9464	0.0136	0.040	0.0437	800-799	0.51	0.46

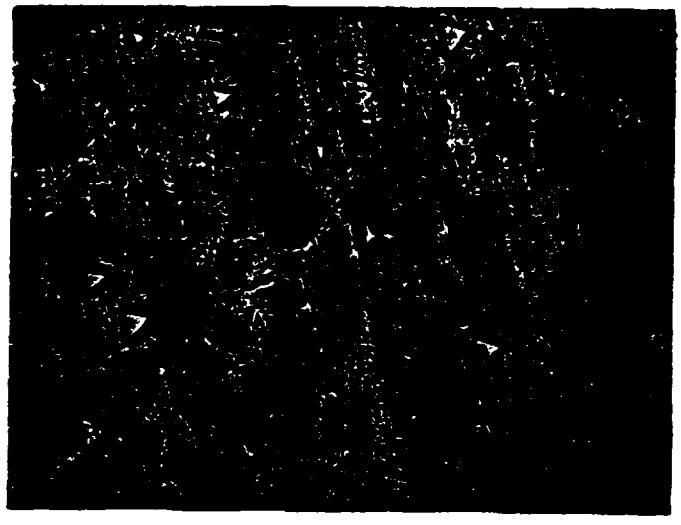

(a) surface

(b) interface

Figure 4.4 Typical layer grown on {111} As GaAs without substrate protection during melt homogenization period.

was protected by another GaAs wafer during the melt equilibration period. The experimental results with this procedure indicate the epitaxial layers grown on {111}As substrate without phosphorus contamination have much improved surfaces and flat interfaces as shown in Figure 4.5.

Double crystal x-ray analysis of {111}As oriented samples shows three different peaks. One such scan is shown in Figure 4.6. The sharpest peak is assumed to be due to the GaAs substrate with a lattice constant of 5.6532Å. The lattice constants calculated for the other peaks are 5.6551Å and 5.6798Å which correspond to GaP fractions of x=0.51 and x=0.45 and energy gaps of E_g=1.90 and 1.82 eV. The FWHM of these peaks are much larger than those observed for the lattice-matched {110} samples.

We are currently investigating conditions for the growth of lattice-matched $Ga_xIn_{1-x}P$ on {211} GaAs substrates. A comparison of the results obtained on {110} and {111}As substrates, however, reveal some interesting features. When these two orientations are grown with the same melt compositions and temperatures, the solid compositions are different. Whether this difference in effective segregation coefficients is due to an orientation or growth rate effect is not known at the present time. As can be seen in Figures 4.2 and 4.4 the {110} growth rate is greater than that for the {111}As layers. In fact the rough surfaces

(a) Nomarski interference photograph of surface

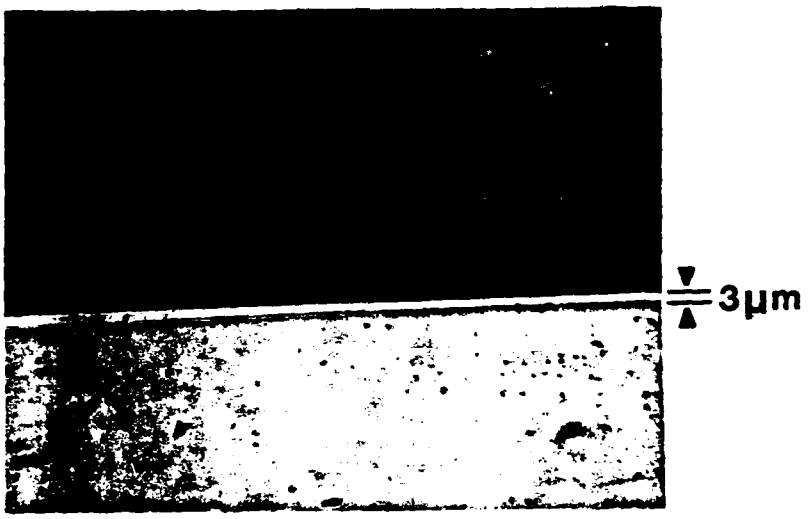

(b) interface

Figure 4.5 Layer grown on {111} As GaAs where substrate is protected during melt homogenization period.

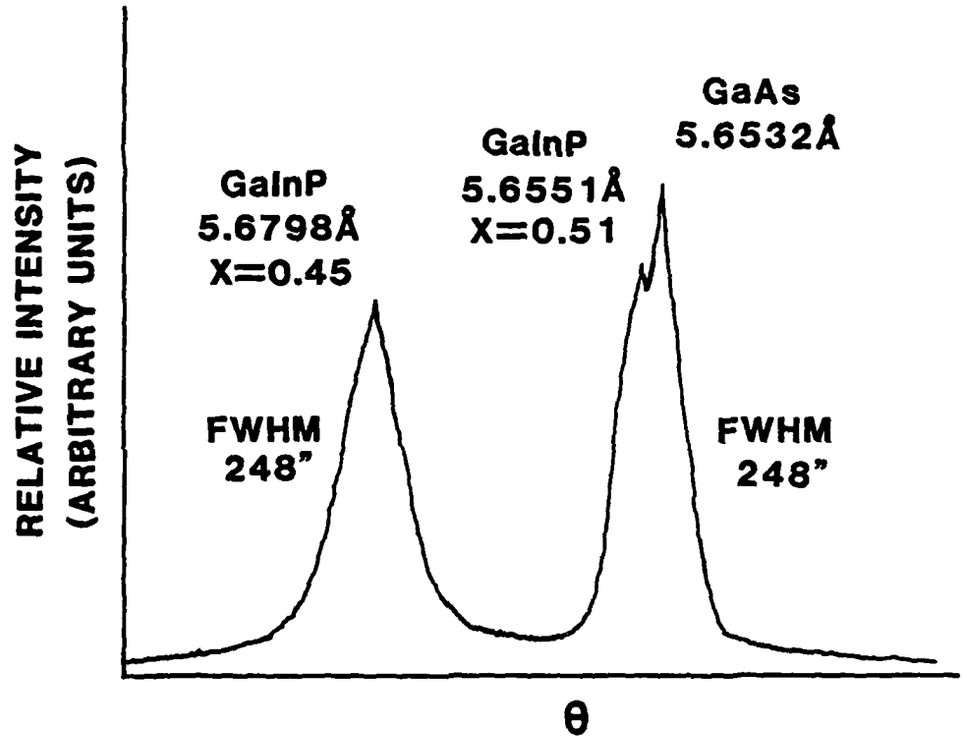

Figure 4.6 Double crystal x-ray analysis of {111} As sample.

observed for the {110} layers are probably the result of a growth rate which is too fast.

Another salient feature is that, for conditions which produce well-matched {110} layers, the {111}As layers appear to be two-phase solid solutions. This is indicated by the two layer peaks in Figure 4.6 and the FWHM of the {110} and {111}As peaks are consistent with this conclusion. That is, the much larger FWHM for the {111}As peaks indicate substantial lattice strain in the {111}As layers. A conclusion which can be made from these preliminary results is that growth of $Ga_xIn_{1-x}P$ on {111}As GaAs substrates is less stable than growth on {110} substrates.

4.3 REFERENCES

1. G.B. Stringfellow, J. Electrochem. Soc. 117, 1301 (1970).
2. A.W. Mabbitt, J. Materials Science 5, 1043 (1970).
3. K. Kajiyama, Japan. J. Appl. Phys. 10, 561 (1971).
4. B.W. Hakki, J. Electrochem. Soc. 118, 1469 (1971).
5. G.B. Stringfellow, P.F. Lindquist, and R.A. Burmeister, J. Electron. Mater. 1, 437 (1972).
6. I. Ohta, M. Kazumar, and I. Tevamoto, Gallium Arsenide and Related Compounds (The Institute of Physics, London, 1981) p.59.
7. A. Lewis, J. of Crystal Growth 53, 530 (1981).
8. C.B. Morrison and S.M. Bedair, J. Appl. Phys. 53, 9058 (1982).
9. T. Sugiura, H. Sugiura, A. Tanaka, and T. Sukegawa, J. of Crystal Growth 49, 559 (1980).
10. W.R. Hitchens, N. Holonyak, M.H. Lee, and J.C. Campbell, J. of Crystal Growth 27, 154 (1974).
11. G. M. Blom, J. Electrochem. Soc. 118, 1834 (1971).
12. H. Asai and K. Oe, J. Appl. Phys. 53, 6849 (1982).

5. PUBLICATIONS

1. G.A. Davis and C.M. Wolfe, "Liquid Phase Epitaxial Growth of $ZnSnP_2$ on GaAs", J. Electrochem. Soc. 130, 1408 (1983).

2. G.A. Davis, M.W. Muller, and C.M. Wolfe, "Antiphase Boundary Suppression in Chalcopyrite on Sphalerite Epitaxy", to be submitted to J. Crystal Growth.

6. PERSONNEL

The personnel who worked on this grant during the first year were:

Prof. C.M. Wolfe, Principal Investigator

Prof. M.W. Muller, Faculty Associate

Mr. Gary A. Davis, Graduate Research Assistant

Ms. S. Julie Hsieh, Graduate Research Assistant

The Graduate Research Assistants have master's degrees and Ms. Hsieh is a doctoral candidate. Mr. Davis has completed his doctoral requirements.

The degree awarded on this grant up to the present time is:

May 1983, Gary A. Davis, Doctor of Science, "Preparation and Properties of $Zn_xCd_{1-x}SnP_2$ Epitaxially Grown on InP and GaAs".

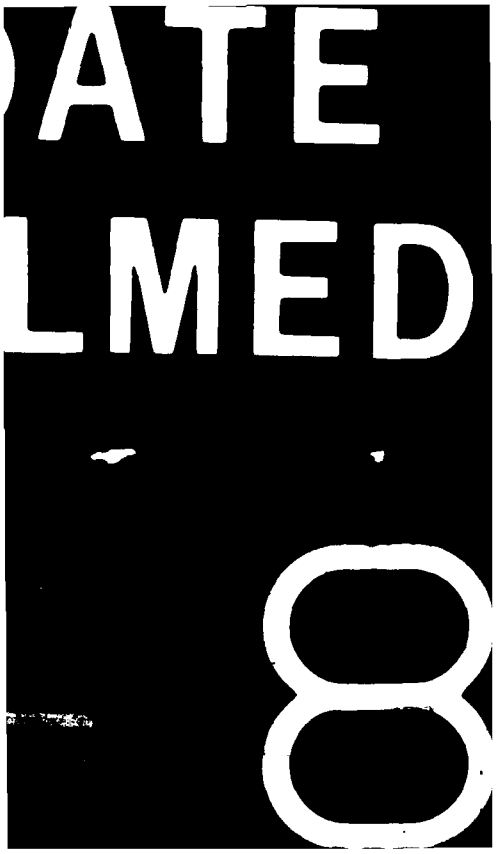
ATE
LMED
8